Dual-color ultraviolet metal-semiconductor-metal AlGaN photodetectors

Mutlu Gökkavas,[a] Serkan Butun, HongBo Yu, Turgut Tut, Bayram Butun, and Ekmel Ozbay

Nanotechnology Research Center, Bilkent University, Bilkent, Ankara 06800, Turkey and Department of Physics, Bilkent University, Bilkent, Ankara 06800, Turkey and Department of Electrical and Electronics Engineering, Bilkent University, Bilkent, Ankara 06800, Turkey

(Received 11 July 2006; accepted 11 August 2006; published online 2 October 2006)

Backilluminated ultraviolet metal-semiconductor-metal photodetectors with different spectral responsivity bands were demonstrated on a single $Al_xGa_{1-x}N$ heterostructure. This was accomplished by the incorporation of an epitaxial filter layer and the recess etching of the surface. The 11 nm full width at half maximum (FWHM) responsivity peak of the detector that was fabricated on the as-grown surface was 0.12 A/W at 310 nm with 10 V bias, whereas the 22 nm FWHM responsivity peak of the detector fabricated on the recess-etched surface was 0.1 A/W at 254 nm with 25 V bias. Both detectors exhibited excellent dark current characteristics with less than 10 fA leakage current. © *2006 American Institute of Physics*. [DOI: 10.1063/1.2358206]

$Al_xGa_{1-x}N$ based solid-state photodetectors have attracted much attention for photodetection in the ultraviolet (UV) spectrum from the near UV to deep UV.[1–3] In the past decade, metal-semiconductor-metal-[4,5] Schottky-[6,7] and *p-i-n*-type[8,9] UV photodetectors have been demonstrated successfully. Ultraviolet detectors have a wide range of applications such as flame detection, biological and chemical analysis, optical communications, and emitter calibration. Multiple narrow-band detectors that offer the ability to analyze separate spectral bands are particularly desirable for fire source and range recognition in order to eliminate false alarms. Existing fire warning systems utilize infrared (IR)/IR,[10] UV/IR, or UV/visible/IR channels. Multispectrum UV detectors would further improve the capabilities of such systems. In addition, such detectors would be advantageous for increased communication capacity in short distance non-line-of-sight optical communication systems. One method of narrow spectral-band detection is the resonant cavity enhancement scheme, which has been utilized for high performance detectors in other wavelength ranges.[11,12] An alternative, which is particularly suited to the $Al_xGa_{1-x}N$ system due to the large absorption coefficient, is to employ absorptive epitaxial filter layers. Similar devices, where the absorptive response of one photodiode acts as a filter for a second vertically integrated Si photodiode, have been employed for wavelength monitoring of laser diodes.[13] In this letter, we report our work on dual-band UV metal-semiconductor-metal (MSM) photodetectors that were fabricated on a single chip.

Metal-semiconductor-metal-type photodetectors simplify the growth and fabrication processes as the necessity for contacts and doped Ohmic layers is eliminated.[14] The dual-color photodetector structure incorporates a built-in epitaxial spectral filter layer sandwiched between two detector active layers; therefore the device is designed for substrate-side illumination. An additional advantage of back side illumination is that semitransparent finger metallization is not necessary, which in turn further simplifies fabrication. Figure 1 is a conceptual drawing of the proposed dual-band UV MSM photodetectors. Detector 2 has the epitaxial layer with the highest band-gap energy (E_{g2}), therefore, the highest Al concentration (x_2). Light that is not absorbed ($h\nu < E_{g2}$) in the active layer of detector 2 travels through a thick spectral filter layer that has an intermediate band-gap energy (E_{gf}) and Al concentration ($x_f < x_2$). All photons with energy $E_{g2} > h\nu > E_{gf}$ are absorbed in the filter layer in the vicinity of the interface with detector 2 layer, while those photons with $h\nu < E_{gf}$ are transmitted through the filter layer. The thickness of the spectral filter layer is such that the photogenerated carriers in this layer recombine before they can diffuse into the E-field of photodetector 1. Therefore, detector 1, which has the lowest Al concentration ($x_1 < x_f$) and the lowest band-gap energy (E_{g1}), only detects light with $E_{gf} > h\nu > E_{g1}$.

The sample in this study was grown on a double-side polished *c*-face (0001) sapphire substrate by low-pressure metal organic chemical vapor deposition. We used hydrogen as the carrier gas, and trimethylaluminum, trimethylgallium, and ammonia (NH_3) were used as the Al, Ga, and N sources, respectively. Prior to the epitaxial growth, sapphire substrates were annealed at 1100 °C for 10 min to remove surface contamination, and subsequently a 15 nm thick AlN nucleation layer was deposited at 550 °C. Thereafter, the reactor temperature was ramped to 1130 °C, pressure was ramped down to 25 mbars, and a 400 nm thick detector 2 layer ($x_2 \approx 0.5$) was grown, followed by another nucleation layer of 15 nm thick AlN at 550 °C in order to prevent dis-

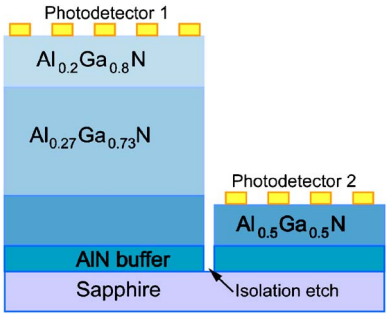

FIG. 1. (Color online) Conceptual schematic of dual-band MSM UV photodetectors.

[a]Electronic mail: mgokkavas@fen.bilkent.edu.tr

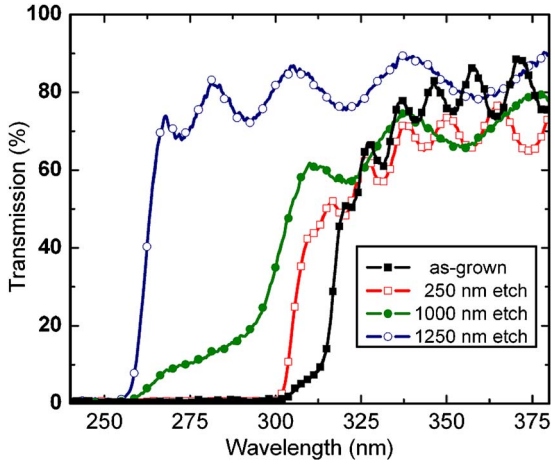

FIG. 2. (Color online) Transmission of the dual-band photodetector sample prior to a surface recess etch and for three different etch depths.

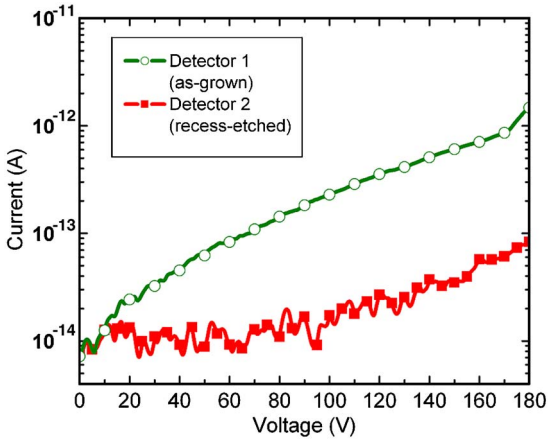

FIG. 3. (Color online) Current-voltage characteristics of 100×100 μm^2 MSM photodetectors with 3 $\mu m/3$ μm finger width/spacing fabricated on the as-grown surface (detector 1) and recess-etched surface (detector 2).

locations and cracks in the subsequent 1 μm thick filter layer ($x_f \approx 0.25$). The growth conditions for the filter layer were as follows: reactor pressure of 50 mbars, growth temperature of 1080 °C, H_2 carrier gas, and growth rate of approximately. 2 μm/h. Finally, the 250 nm thick detector 1 layer ($x_1 \approx 0.2$) was grown at 1080 °C.

For a better understanding of the alloy compositions and layer thicknesses, epitaxial material was removed progressively by CCl_2F_2 based reactive ion etching (RIE). Figure 2 shows the spectral transmission measurements of the wafer prior to the surface recess etch, and for three different etch depths. The as-grown wafer exhibited a sharp cut-off at 315 nm, which corresponds to an Al concentration of approximately 20% for the ~250 nm thick detector 1 layer ($x_1=0.2$). An absorption tail between 301 and 315 nm was also observed due to a slight transmission through the $Al_{0.2}Ga_{0.8}N$ layer. After a RIE process removing 250 nm of epitaxial material, the transmission exhibited a sharp cutoff at 301 nm, which indicates a 27% Al concentration for the 1 μm thick filter layer ($x_f=0.27$). For a total etch depth of 1000 nm, a partial transmission is observed between 259 and 301 nm. This is because the remaining $Al_{0.27}Ga_{0.73}N$ layer is not thick enough to absorb the entire incident light. Finally, when 1250 nm of material was removed, the sample exhibited a sharp cutoff at 259 nm, which indicates a 50% Al concentration for the 400 nm thick high-Al-concentration detector 2 layer ($x_2=0.5$).

For the fabrication of the dual-color photodetectors, a 1×2 cm^2 piece was cut; half of the sample was covered with photoresist and subsequently RIE in several steps. Utilizing the transmission data, the etch process was stopped when the detector 2 layer was reached. On the etched and as-grown parts of the sample, MSM photodetectors were fabricated in a class-100 clean room environment. The width and the spacing of the interdigitated 100 Å Ni/5000 Å Au fingers varied between 1.5 and 5 μm. The 100×100 and 200×200 μm^2 device active areas were isolated by a deep mesa etch, and the 100×200 μm^2 probe pads were placed on the sapphire substrate.

Dark current was measured using low-noise triaxial cables in a grounded shielded cage by a Keithley 6517A high-resistance electrometer. Figure 3 shows the measured dark current for the MSM photodetectors fabricated on the as-grown and 1.3 μm recess-etched surfaces of the wafer. Both detectors were 100×100 μm^2 area devices with 3 $\mu m/3$ μm finger width/spacing. The dark current of the device fabricated on the recess-etched surface (detector 2) was below the dark current of the device fabricated on the as-grown surface (detector 1) with an order of difference at the higher end of the voltage range. The dark currents at 0 V bias were 9 and 7 fA for detectors 1 and 2, respectively. Both devices exhibited good breakdown characteristics. Soft breakdown occurred at 180 V for detector 1, whereas no sign of breakdown was observed for detector 2. The improved dark current characteristics of the recess-etched device can be attributed mainly to the higher Al concentration. Furthermore, this better electrical performance also indicates the high quality of the epitaxial layers, with no significant morphological or contact degradation following prolonged RIE.

Spectral photocurrent characteristics of the fabricated devices were measured by way of a Xe lamp and monochromator assembly. The narrow spectral output of the monochromator was modulated by an optical chopper, coupled into a multimode UV-enhanced fiber, and delivered through the substrate (back side illumination) of the device under test on a probe station. The resulting photocurrent was recorded as a function of wavelength using a lock-in amplifier. The spectral power density of the light at the output of the fiber was measured by a NIST-traceable calibrated Si photodetector. For photocurrent measurements, 200×200 μm^2 area devices with 3 $\mu m/3$ μm finger width/spacing were used. The responsivity of both devices in the 200–500 nm spectral range is plotted in Fig. 4 in logarithmic scale, where the inset shows the same data in linear scale. Both devices exhibited bias-dependent responsivity that is typical of MSM detectors, and the bias values were chosen such that the peak responsivities would be comparable. For the detector fabricated on the as-grown surface (detector 1), the peak of the response is 0.12 A/W for a 10 V bias, which occurs at 310 nm. In comparison, the peak responsivity of the recess-etched detector (detector 2) is 0.1 A/W at 254 nm for a 25 V bias. The full widths at half maximum (FWHMs) of the responsivity peak were 11 and 22 nm for detectors 1 and 2, respectively. Detector 1 response drops sharply below 300 nm for nearly five orders of magnitude. This is because of the 1 μm thick $Al_{0.27}Ga_{0.73}N$ layer, which acts as an absorptive spectral filter. The slight gradual increase in the response towards lower wavelengths is not a measured in-

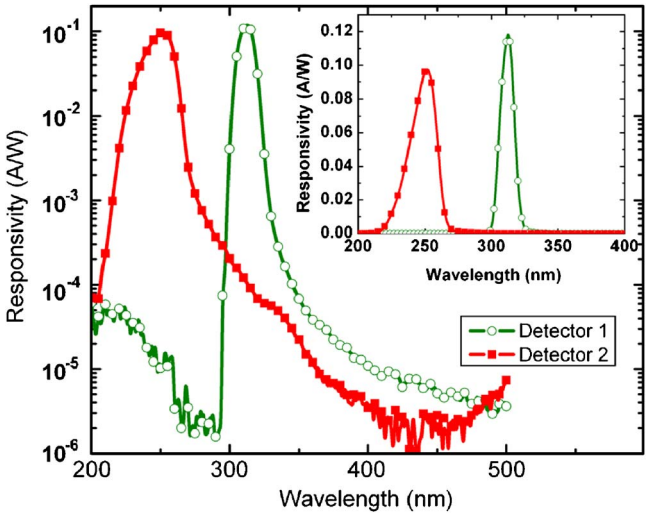

FIG. 4. (Color online) Spectral responsivity characteristics of 200 $\times 200$ μm^2 dual-band MSM photodetectors with 3 $\mu m/3$ μm finger width/spacing fabricated on the as-grown surface (detector 1) and recess-etched surface (detector 2).

crease in the photocurrent; it is due to a decrease in the dynamic range of our measurement setup. The increase towards 200 nm merely reflects an increase in the noise floor. Nevertheless, detector 1 rejects light in the detector 2 operation band with more than four orders of magnitude, whereas detector 2 rejects light in the detector 1 operation band with more than three orders of magnitude. Furthermore, both detectors reject visible light extremely well, with more than four orders of rejection at 500 nm. The slight increase in the detector 2 response between 450 and 500 nm is due to higher order leakage from the monochromator.

In conclusion, we fabricated and tested two UV MSM photodetectors with separate spectral bands on the same chip. This was accomplished by the incorporation of an epitaxial filter layer and the recess etching of the surface. The 11 nm FWHM responsivity peak of the detector that was fabricated on the as-grown surface (detector 1) was 0.12 A/W at 310 nm with a 10 V bias, whereas the 22 nm FWHM responsivity peak of the detector that was fabricated on the recess-etched surface (detector 2) was 0.1 A/W at 254 nm with a 25 V bias. Detector 1 rejected the light in the detector 2 operation band with more than four orders of magnitude, and detector 2 rejected light in the detector 1 operation band with more than three orders of magnitude. Both detectors exhibited excellent dark current characteristics with less than 10 fA leakage at 0 V bias. The method described in this letter is expandable to a higher number of detectors in a wider wavelength range when a larger number of epitaxial layers are employed.

This work was supported by EU NOE-PHOREMOST, by EU NOE-METAMORPHOSE, and by TUBITAK under Project Nos. 104E090, 105E066, and 105A005. One of the authors (E.O.) acknowledges partial support from the Turkish Academy of Sciences.

[1] M. Razeghi and A. Rogalsky, J. Appl. Phys. **79**, 7433 (1996).
[2] E. Monroy, F. Omnes, and F. Calle, Semicond. Sci. Technol. **18**, R33 (2003).
[3] M. A. Khan, M. Shatalov, H. P. Maruska, H. M. Wang, and E. Kuokstis, Jpn. J. Appl. Phys., Part 1 **44**, 7191 (2005).
[4] T. Li, D. J. H. Lambert, A. L. Beck, C. J. Collins, B. Yang, J. M. M. Wong, U. Chowdhury, R. D. Dupuis, and J. C. Campbell, Electron. Lett. **36**, 1581 (2000).
[5] J. Y. Duboz, J. L. Reverchon, D. Adam, B. Damilano, N. Grandjean, F. Semond, and J. Massies, J. Appl. Phys. **92**, 5602 (2002).
[6] N. Biyikli, I. Kimukin, O. Aytur, M. Gökkavas, M. S. Unlu, and E. Ozbay, Appl. Phys. Lett. **79**, 2838 (2001).
[7] N. Biyikli, I. Kimukin, T. Tut, O. Aytur, and E. Ozbay, Appl. Phys. Lett. **81**, 3272 (2002).
[8] C. J. Collins, U. Chowdhury, M. M. Wong, B. Yang, A. L. Beck, R. D. Dupuis, and J. C. Campbell, Appl. Phys. Lett. **80**, 3754 (2002).
[9] U. Chowdhury, M. M. Wong, C. J. Collins, B. Yang, J. C. Denyszyn, J. C. Campbell, and D. Dupuis, J. Cryst. Growth **248**, 552 (2003).
[10] M. B. Reine, P. W. Norton, R. Starr, M. H. Weiler, M. Kestigian, B. L. Musicant, P. Mitra, T. Schimert, F. C. Case, I. B. Bhat, H. Ehsani, and V. Rao, J. Electron. Mater. **24**, 669 (1995).
[11] B. M. Onat, M. Gökkavas, E. Ozbay, E. P. Ata, E. Towe, and M. S. Unlu, IEEE Photonics Technol. Lett. **10**, 707 (1998).
[12] M. S. Unlu, M. Gökkavas, B. M. Onat, E. P. Ata, E. Ozbay, R. P. Mirin, K. J. Knopp, K. A. Bertness, and D. H. Christensen, Appl. Phys. Lett. **72**, 2727 (1998).
[13] S. Roy, S. Chaudhuri, and C. S. Unnikrishnan, Am. J. Phys. **73**, 571 (2005).
[14] E. Monroy, F. Calle, E. Munoz, and F. Omnes, Appl. Phys. Lett. **74**, 3401 (1999).